

Electronic structure calculations in ordered and disordered solids with spiral magnetic order

S. Mankovsky,¹ G. H. Fecher,² and H. Ebert¹

¹*Department of Chemistry, Physical Chemistry, Ludwig Maximilian University, Butenandtstrasse 11, D-81377 Munich, Germany*

²*Institut für Anorganische Chemie und Analytische Chemie, Johannes-Gutenberg-Universität, D-55099 Mainz, Germany*

(Received 14 December 2010; revised manuscript received 9 February 2011; published 1 April 2011)

A scheme to calculate the electronic structure of systems having a spiral magnetic structure is presented. The approach is based on the Korringa-Kohn-Rostoker Green's function formalism which allows, in combination with the coherent potential approximation alloy theory, dealing with chemically disordered materials. It is applied to the magnetic random alloys $\text{Fe}_x\text{Ni}_{1-x}$, $\text{Fe}_x\text{Co}_{1-x}$, and $\text{Fe}_x\text{Mn}_{1-x}$. For these systems the stability of their magnetic structure was analyzed. For $\text{Fe}_x\text{Ni}_{1-x}$ the spin stiffness for was determined as a function of concentration that was found in satisfying agreement with experiment. Performing spin spiral calculations the longitudinal momentum-dependent magnetic susceptibility was calculated for pure elemental systems (Cr, Ni) in the nonmagnetic state as well as for random alloys ($\text{Ag}_x\text{Pt}_{1-x}$). The obtained susceptibility was used to analyze the stability of the paramagnetic state of these systems.

DOI: [10.1103/PhysRevB.83.144401](https://doi.org/10.1103/PhysRevB.83.144401)

PACS number(s): 71.15.-m, 71.55.Ak, 75.30.Ds

I. INTRODUCTION

The use of symmetry properties of solids for calculations of their electronic structure is a very efficient way to reduce the computational effort required for the solution of the problem. In particular, the single-particle electronic states of paramagnetic or collinear magnetic infinite solids can be effectively found by solving the corresponding Kohn-Sham-Dirac equation making use of the Bloch theorem. Dealing with systems exhibiting noncollinear magnetic structure, the electronic structure problem becomes much more complicated because of broken symmetry (in general, both translational and rotational), leading to an increase of the unit cell of a system and a corresponding increase of the required computational effort.

Sandraskii introduced an approach that allows the calculation of the electronic structure of systems with spiral magnetic structures in an efficient way.^{1,2} This approach is based on the symmetry properties of spin spiral structures as investigated by Brinkman and Elliot^{3,4} and Herring⁵ and allows dealing with long-period noncollinear magnetic structures, avoiding the use of big unit cells in electronic structure calculations.⁶ This makes it an efficient tool for the analysis of the stability of various noncollinear magnetic structures with different translation periods, as for example demonstrated by Mryasov *et al.*⁷ for the investigation of the magnetic structure of fcc Fe.

In the case of systems with a collinear magnetic structure as a ground state spin spirals can be treated as transverse spin fluctuations in the adiabatic approximation. The energy dispersion of such fluctuations $\Delta E(\vec{q})$ gives access to the spin stiffness and exchange coupling constants of a system and in this way to the spin excitation spectrum as well as finite temperature magnetism.⁸⁻¹⁰ An important feature of spin spiral calculations is that they account for longitudinal fluctuations of the magnetic moment. This leads to more reliable results for $\Delta E(\vec{q})$ compared to those obtained using the non-self-consistent force-theorem approach.

As was pointed out by Sandratskii and Kübler¹¹ the technique for spin spiral calculations can be used for calculations of the static ($\omega = 0$) momentum-resolved longitudinal

magnetic susceptibility. Until now only few corresponding *ab initio* calculations have been presented in the literature. In most cases the static q -dependent magnetic susceptibility was calculated using perturbation theory¹² or performing supercell calculations.¹³ The spin spiral method, on the other hand, allows one to perform self-consistent calculations of the magnetic susceptibility, avoiding the supercell concept.¹¹

All spin spiral calculations have been done so far using the ASW^{10,14,15} or LMTO^{7,8} band structure methods. These methods use Bloch-function basis sets to represent the solution of the Kohn-Sham equation and for that reason are restricted to ordered materials concerning the application. The use of multiple scattering theory in combination with CPA (coherent potential approximation) alloy theory, on the other hand, substantially extends the variety of materials which can be investigated by giving access to systems without chemical order. This feature of the CPA was already exploited by Staunton *et al.*¹² who worked out a corresponding formulation of linear response formalism. Here we present a self-consistent implementation of the spin spiral approach within the Korringa-Kohn-Rostoker (KKR) Green's function band structure method.¹⁶ We will show the results of calculations for different systems focusing on disordered alloys.

II. THEORETICAL BACKGROUND

When dealing with the electronic structure of solid state systems having a spiral magnetic structure rotations can be applied independently to the spin and spatial parts of the electronic wave function if spin-orbit coupling (SOC) is neglected. Using a spin-diagonal form of the exchange-correlation potential in the local frame of reference of an atom site, the Kohn-Sham equation for the spinor wave function $\psi(\vec{r})$ can be written in the form

$$\left[-\nabla^2 \begin{pmatrix} 1 & 0 \\ 0 & 1 \end{pmatrix} + \sum_{nv} U_{nv}^\dagger(\theta_v, \phi_v) \begin{pmatrix} V_{nv}^+(\vec{r}) & 0 \\ 0 & V_{nv}^-(\vec{r}) \end{pmatrix} U_{nv}(\theta_v, \phi_v) \right] \psi(\vec{r}) = E \psi(\vec{r}). \quad (1)$$

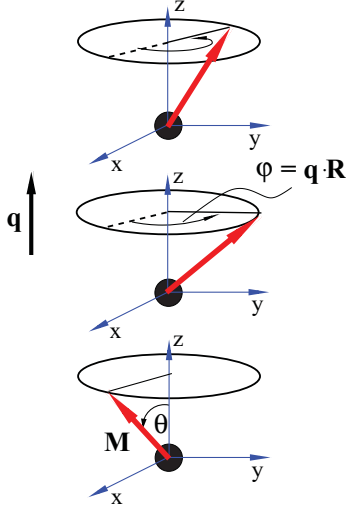


FIG. 1. (Color online) Geometry of a spin spiral with the wave vector \vec{q} along the z direction.

Here \vec{r}_v denotes a position of an atom in a unit cell, \vec{R}_n is a Bravais lattice vector, and U_{nv} is a spin transformation matrix that connects the global frame of reference of the crystal to the local frame of the atom site at $\vec{r}_v + \vec{R}_n$ that has its magnetic moment tilted away from the global z direction. The transformation U_{nv} is characterized by the Euler angles $\theta_{n,v}$ and $\phi_{n,v}$ as shown in Fig. 1 for the case of a spin spiral.

As was shown by Sandratskii, considering a spin spiral structure, Eq. (1) can be easily dealt with using the properties of spin space groups (SSG)³⁻⁵ allowing independent transformations within the spin and space subspaces. The spin spirals characterized by the wave vector \vec{q} angles θ_v and ϕ_v are represented by the expression

$$\vec{m}_n^v = m^v [\cos(\vec{q} \cdot \vec{R}_n + \phi_v) \sin \theta_v, \sin(\vec{q} \cdot \vec{R}_n + \phi_v) \sin \theta_v, \cos \theta_v],$$

defining the spin direction at every site (n, v) of the lattice with m^v the magnitude of the magnetic moment on site v within the unit cell. Assuming a collinear alignment of the spin density within the atomic cell at (n, v) , it is natural to use a local frame of reference with its z axis oriented along \vec{m}_n^v . The corresponding transformation matrices U_{nv} occurring in Eq. (1) can be written as a product of two independent rotation matrices $U_{nv}^{\vec{q}} = U_n(\theta_v, \phi_v, \vec{q}) = U_v(\theta_v, \phi_v) U_{\vec{q}\vec{R}_n}$ where the matrix $U_{\vec{q}\vec{R}_n}$ depends only on the translation vector \vec{R}_n .^{1,2}

$$U_n(\theta_v, \phi_v, \vec{q}) = \begin{pmatrix} \cos \frac{\theta_v}{2} & \sin \frac{\theta_v}{2} \\ -\sin \frac{\theta_v}{2} & \cos \frac{\theta_v}{2} \end{pmatrix} \begin{pmatrix} e^{\frac{i}{2}\phi_v} & 0 \\ 0 & e^{-\frac{i}{2}\phi_v} \end{pmatrix} \times \begin{pmatrix} e^{\frac{i}{2}(\vec{q} \cdot \vec{R}_n)} & 0 \\ 0 & e^{-\frac{i}{2}(\vec{q} \cdot \vec{R}_n)} \end{pmatrix} = U_v U_{\vec{q}\vec{R}_n}. \quad (2)$$

Instead of solving the Kohn-Sham Eq. (1) for the eigen functions and values the electronic structure can be represented in terms of the corresponding Green's function. Within multiple scattering theory the Green's function is represented in real space by the scattering path operator $\underline{\tau}^{nn'}$ together with the regular $Z_{\Lambda_1}^n(\vec{r}, E)$ and irregular $J_{\Lambda_1}^n(\vec{r}, E)$ solutions of the

single-site Kohn-Sham equation referring to the local frame of reference:

$$G^+(\vec{r}, \vec{r}', E) = \sum_{\Lambda_1 \Lambda_2} Z_{\Lambda_1}^n(\vec{r}, E) \tau_{\Lambda_1 \Lambda_2}^{nn'}(E) Z_{\Lambda_2}^{n' \times}(\vec{r}', E) - \sum_{\Lambda_1} [Z_{\Lambda_1}^n(\vec{r}, E) J_{\Lambda_1}^{n \times}(\vec{r}', E) \Theta(r' - r) \times J_{\Lambda_1}^n(\vec{r}, E) Z_{\Lambda_1}^{n \times}(\vec{r}', E) \Theta(r - r')] \delta_{nn'}. \quad (3)$$

The scattering path operator is defined by its equation of motion:

$$\underline{\tau}^{nv n' v'} = \underline{t}^{nv} \delta_{nn' v' v'} + \underline{t}^{nv} \sum_{kp}' \underline{G}^{nq m \mu} \underline{\tau}^{m \mu n' v'}, \quad (4)$$

where \underline{t}^{nv} and $\underline{G}^{nq m \mu}$ are the single-site t matrix and free-electron propagator, respectively, which are both expressed with respect to a common global frame of reference. Equation (4) has the formal solution

$$\underline{\tau} = [\underline{t}^{-1} - \underline{G}]^{-1}. \quad (5)$$

In Eqs. (4) and (5) the underline indicates matrices in the (l, m) representation while the double underline indicates supermatrices including the site index. In the case of a collinear magnetic structure the local and global frames of reference coincide. This implies that Eq. (5) gives immediately the solution with respect to the local frame of reference. For infinite systems having a regular periodic lattice a solution to Eq. (4) can be obtained by Fourier transformation instead of using the real space expression given in Eq. (5).

For noncollinear magnetic solids with a periodic lattice structure one can solve Eq. (4) as for collinear systems but using an extended supercell. The size of the corresponding supercell is determined by the period of magnetic structure. All atoms within the cell are in general inequivalent and have their own local frame of reference. Therefore supercell calculations can be rather time consuming in particular for magnetic structures having a long period.

However, as pointed by various authors³⁻⁵ use of symmetry allows one to simplify the problem substantially. Spiral magnetic structures transform according to the group of generalized translations that are characterized by the wave vector \vec{q} and represented by the matrices $U_{\vec{q}\vec{R}_n}$ [Eq. (2)]. This implies in particular that the matrices $U_{\vec{q}\vec{R}_n}$ allow the expression of the single-site t matrix t^{nv} at site (nv) to that at site $(0v)$. This symmetry property allows one to write the scattering path operator referring to the global frame of reference as follows:

$$\tau^{nv n' v'} = t^{nv} \delta_{nn' v' v'} + t^{nv} \sum_{m\mu}' G^{nv m \mu} \tau^{m \mu n' v'} = U_{nv}^{\vec{q} \dagger} \tilde{\tau}^{nv} U_{nv}^{\vec{q}} \delta_{nn' v' v'} + U_{nv}^{\vec{q} \dagger} \tilde{\tau}^{nv} U_{nv}^{\vec{q}} \sum_{m\mu}' G^{nv m \mu} \tau^{m \mu n' v'}. \quad (6)$$

This allows one to find the scattering path operator and from this the Green's function in the local frame of reference of the each atom, solving the equation

$$\tilde{\tau}^{nv n' v'} = U_{nv}^{\vec{q}} \underline{\tau}^{nv n' v'} U_{nv}^{\vec{q} \dagger} = \tilde{t}^{nv} \delta_{nn' v' v'} + \tilde{t}^{nv} \sum_{m\mu}' U_{nv}^{\vec{q}} \underline{G}^{nv m \mu} U_{m\mu}^{\vec{q} \dagger} U_{m\mu}^{\vec{q}} \underline{\tau}^{m \mu n' v'} U_{n' v'}^{\vec{q} \dagger} \quad (7)$$

$$= \tilde{t}^v \delta_{nv n'v'} + \tilde{t}^v \sum_{m\mu} U_{nv}^{\tilde{q}} \underbrace{G^{nv m\mu}}_{\tilde{G}^{nv m\mu}} U_{m\mu}^{\tilde{q}\dagger} \underbrace{U_{m\mu}^{\tilde{q}} \tau^{m\mu n'v'}}_{\tilde{\tau}^{m\mu n'v'}} U_{n'v'}^{\tilde{q}\dagger}, \quad (8)$$

where the tilde indicates matrices which refer to the local frame of reference.

In the last line of Eq. (8) use has been made that the single-site t matrices \tilde{t}^{nv} do not depend on the lattice index n but only on the site index v in the unit cell. As a consequence, the multiple scattering problem can be solved as for the case of collinear magnetic structures by Fourier transformation of the equation of motion for the scattering path operator. This leads to its representation in reciprocal space according to

$$\tilde{\tau}(\vec{k}, E) = [\tilde{t}^{-1}(E) - \tilde{G}(\vec{k})]^{-1}. \quad (9)$$

The structural Green's function referring to the local frame of reference can be determined as follows:

$$\begin{aligned} \tilde{G}^{vv'}(\vec{k}) &= \frac{1}{N} \sum_{nn'} e^{-i\vec{k} \cdot (\vec{R}_n - \vec{R}_{n'})} \tilde{G}^{nn'v'v} \\ &= \frac{1}{N} \sum_{nn'} e^{-i\vec{k} \cdot (\vec{R}_n - \vec{R}_{n'})} U_{nv}^{\tilde{q}} \tilde{G}^{nn'v'v'} U_{n'v'}^{\tilde{q}\dagger} \\ &= U_v \begin{pmatrix} \tilde{G}^{vv'}(\vec{k} - \frac{1}{2}\vec{q}) & 0 \\ 0 & \tilde{G}^{vv'}(\vec{k} + \frac{1}{2}\vec{q}) \end{pmatrix} U_v^\dagger \\ &= U_v \tilde{G}_q^{vv'}(\vec{k}) U_v^\dagger. \end{aligned} \quad (10)$$

Here $\tilde{G}^{vv'}(\vec{k})$ is a structural Green's function for one spin channel represented in the global frame of reference.

The charge distribution within the central unit cell $n = 0$ is determined by the cell-diagonal scattering path operator $\tilde{\tau}^{00}$ which can be found by the Brillouin zone integral

$$\begin{aligned} \tilde{\tau}^{00} &= \frac{1}{\Omega_{\text{BZ}}} \int_{\Omega_{\text{BZ}}} d^3k [\tilde{t}^{-1} - \tilde{G}(\vec{k})]^{-1} \\ &= U_0^\dagger \frac{1}{\Omega_{\text{BZ}}} \int_{\Omega_{\text{BZ}}} d^3k [\tilde{t}^{-1} - \tilde{G}_q(\vec{k})]^{-1} U_0 \\ &= U_0^\dagger \tau^{00} U_0, \end{aligned} \quad (11)$$

where U_0 is the transformation matrix diagonalizing the potentials as well as t matrices with respect to spin within the central unit cell.

To perform calculations for disordered alloys the CPA (coherent potential approximation) alloy theory^{17,18} is used. In the case of a spin spiral system the CPA medium is represented in the global frame of reference by the effective single-site scattering matrix \tilde{t}^C and the scattering path operator obtained from the expression

$$\tilde{\tau}^{00,C}(E) = \frac{1}{\Omega_{\text{BZ}}} \int_{\Omega_{\text{BZ}}} d^3k [(\tilde{t}^C(E))^{-1} - \tilde{G}(\vec{k}, E)]^{-1}. \quad (12)$$

The corresponding element projected scattering path operators are obtained from these via

$$\tilde{\tau}^{00,\alpha} = \tilde{\tau}^{00,C} \tilde{D}^\alpha, \quad (13)$$

with

$$\tilde{D}^\alpha = [1 + (\tilde{t}^\alpha)^{-1} - (\tilde{t}^C)^{-1}] \tilde{\tau}^{00,C}]^{-1}. \quad (14)$$

Of course dealing with materials with a pronounced short-range order effect one has to go beyond the CPA theory. In this case one can use either the nonlocal CPA (NL CPA) method¹⁹ or the supercell method in the framework of the special quasirandom structures.²⁰ Note however that the use of supercells needs an additional optimization of the magnetic structure within the cell. The approach developed for calculations of noncollinear spin spiral structures can be used for investigations on the longitudinal magnetic susceptibility as a function of the wave vector \vec{q} .¹¹ This approach allows one to avoid the use of perturbation theory and can be applied to magnetic as well as nonmagnetic systems. In the following we focus on materials in their nonmagnetic state which may exhibit paramagnetism (Ag, Pt_{1-x}), ferromagnetism (Ni), or antiferromagnetism (Cr) in their ground state. For this purpose we specify a spiral external magnetic field to be perpendicular to the direction of the wave vector \vec{q} (i.e., $\theta = 90^\circ$):

$$\vec{B}_n^{\text{ext}} = B_0 [\cos(\vec{q} \cdot \vec{R}_n), \sin(\vec{q} \cdot \vec{R}_n), 0].$$

In this case the potential energy term in the Kohn-Sham equation [see Eq. (1)] is given by

$$\left[\sum_{nv} U_{nv}^\dagger(\theta_v, \phi_v) \begin{pmatrix} V_{nv}(\vec{r}) - \mu_B \vec{B}_n^{\text{ext}} - \Delta V_{n,v}^{\text{xc}}(\vec{r}) \\ 0 \end{pmatrix} U_{nv}(\theta_v, \phi_v) \right]. \quad (15)$$

A self-consistent calculation based on Eq. (15) gives the spin magnetic moment induced by the external magnetic field. The \vec{q} -dependent external magnetic field should be taken small enough to be considered as a perturbation. In this case, assuming a linear response to be the leading term of the response function the corresponding magnetic susceptibility can be derived from the expression

$$\chi(\vec{q}) = \frac{m_{\text{ind}}(\vec{q})}{B_0}. \quad (16)$$

Suppressing the spin-dependent part of the exchange-correlation potential [$\Delta V_{n,v}^{\text{xc}}(\vec{r}) = 0$], one can calculate the unenhanced spin susceptibility $\chi^0(\vec{q})$. Otherwise, Eq. (16) gives the enhanced longitudinal magnetic susceptibility $\chi(\vec{q})$, represented in linear response theory for uniform system by the expression

$$\chi(\vec{q}) = \frac{\chi^0(\vec{q})}{1 - I(\vec{q})\chi^0(\vec{q})}, \quad (17)$$

with $I(\vec{q})$ the exchange integral responsible for the enhancement of the magnetic susceptibility (see, for example, Refs. 10 and 21). In case of a paramagnetic ground state the magnetic susceptibility $\chi(\vec{q})$ is positive for all values of \vec{q} . For other cases the denominator in Eq. (17) may become zero or even negative. This singular behavior of the susceptibility obviously indicates an instability of the paramagnetic state toward a transition to spontaneous formation of ferromagnetic or antiferromagnetic order.

III. RESULTS

A. Spin spiral structure in alloys

In the following several applications of the scheme introduced above are presented that focus on disordered alloys to demonstrate the flexibility of the multiple scattering formalism when dealing with spin spiral systems. Corresponding calculations have been performed for alloys having fcc ($\text{Fe}_x\text{Ni}_{1-x}$ and $\text{Fe}_x\text{Mn}_{1-x}$) and bcc ($\text{Fe}_x\text{Co}_{1-x}$) lattice structure.

For all calculations the angle θ has been chosen to be 90° . For this spin geometry, the spin spiral with $\vec{q} = \frac{\pi}{a}(0,0,1)$ corresponds to a spin configuration where the first neighbor atoms in the (001) direction have an antiparallel (AFM) spin alignment, while $\vec{q} = \vec{0}$ implies a parallel (FM) orientation.

1. The disordered alloy system $\text{Fe}_x\text{Ni}_{1-x}$

Figure 2(a) shows the energy of the disordered $\text{Fe}_x\text{Ni}_{1-x}$ alloy system with a spin spiral structure as a function of the wave vector \vec{q} . For all concentrations the minimum of the energy is found for $\vec{q} = \vec{0}$, implying that the ferromagnetic structure is a more stable configuration than noncollinear structures characterized by wave vectors along the (001) direction.

As can be seen from Fig. 2(b), the local magnetic moment of Ni in pure Ni drops down to $m = 0$ at the wave vector $\vec{q}_c \approx \frac{\pi}{a}(0,0,0.5)$ and the system becomes paramagnetic. This is well known behavior of the magnetic moment in Ni which has been investigated by different authors.^{9,25–27} In terms of the Stoner theory of ferromagnetism (see, e.g., Ref. 10) this means that the criterion for the instability of the paramagnetic state is satisfied only for small wave vectors, while above \vec{q}_c the paramagnetic (PM) state should be the most stable state of the system. The criterion for the instability of the PM state will be discussed below in more detail.

Adding only small amounts of Fe to Ni leads obviously to a nonzero magnetic moment per unit cell at all values of wave vector \vec{q} . This is caused by the large magnetic moment of Fe which depends only slightly on the wave vector. Figure 2(b) shows that the Ni magnetic moment, in contrast to that of Fe, varies rather rapidly with increasing wave vector and changes sign at $\vec{q} \approx \frac{\pi}{a}(0,0,0.6)$. This means that in the vicinity of the ground state of the alloys ($\vec{q} = \vec{0}$) the magnetic moments of Fe and Ni atoms prefer to have parallel alignment, while close to $\vec{q} = \frac{\pi}{a}(0,0,1)$ [AFM structure along (0,0,1) direction] the more favorable orientation of the Fe and Ni moments is antiparallel (AP). Nevertheless, even for small Fe concentrations, the total magnetic moment is determined by the dominating moment of Fe. As a result, the alloy system exhibits effectively a ferromagnetic behavior for all wave vectors, as one can see in Fig. 2.

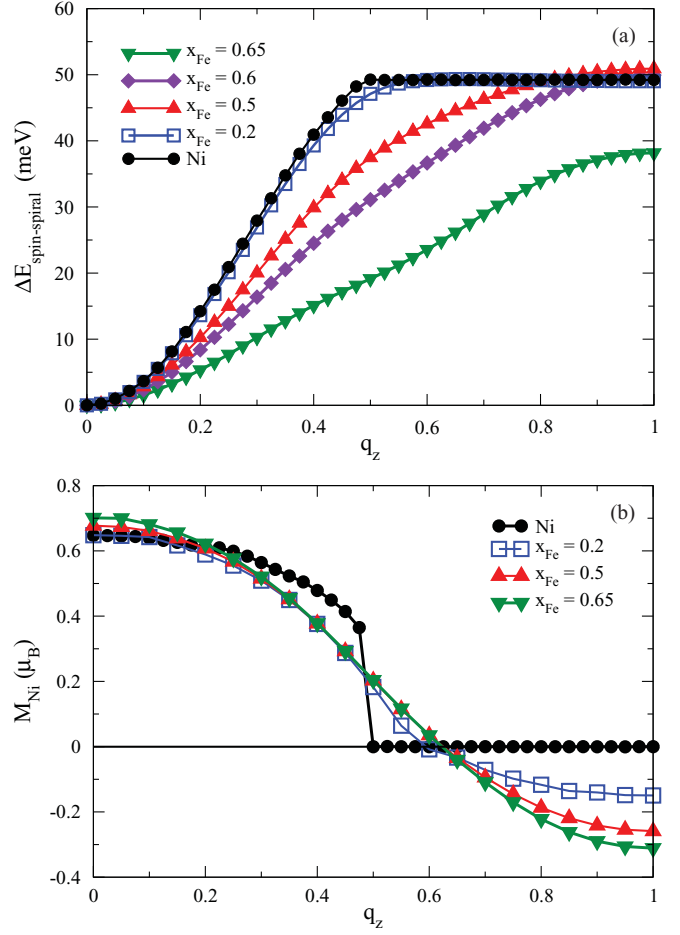


FIG. 2. (Color online) (a) The energy of spin spiral magnetic structure in $\text{Fe}_x\text{Ni}_{1-x}$ alloys. (b) Local magnetic moments on Ni atoms as a function of the wave vector $\vec{q} = \frac{\pi}{a}(0,0,q_z)$.

The energy difference between the spin spiral states with $\vec{q} = \vec{0}$ and $\vec{q} = \frac{\pi}{a}(0,0,1)$ remains almost unchanged up to the Fe concentration $x_{\text{Fe}} \approx 0.6$, and changes nearly by 20% when approaching $x_{\text{Fe}} \approx 0.65$. On the other hand, the spin-stiffness constant deduced from the energy dispersion curves decreases continuously with the increase of Fe content as can be seen from Fig. 3. This figure also shows that the calculations reproduce the available experimental data for the spin-stiffness constant fairly well, although they seem to be slightly too high. This difference can be partially attributed to the conditions of the experiment as, e.g., polycrystallinity of the samples and a finite temperature. The results for the spin stiffness constant D of pure Ni can be compared with theoretical results obtained by other authors who used the exchange coupling parameters calculated within the magnetic force theorem approach:²⁸ $756 \text{ meV} \times \text{\AA}^2$,²⁹ $740 \text{ meV} \times \text{\AA}^2$,³⁰ $527 \text{ meV} \times \text{\AA}^2$.³¹

2. The disordered alloy $\text{Fe}_{0.5}\text{Co}_{0.5}$

The change of sign of the magnetic moment observed for $\text{Fe}_x\text{Ni}_{1-x}$ alloys for one of the alloy components upon variation of the wave vector becomes even more pronounced in bcc $\text{Fe}_{0.5}\text{Co}_{0.5}$ and fcc $\text{Fe}_{0.5}\text{Mn}_{0.5}$ alloys. Disordered bcc $\text{Fe}_{0.5}\text{Co}_{0.5}$ has a ferromagnetic ground state. The spin spiral energy shown in Fig. 4(a) increases with wave vector confirming the stability

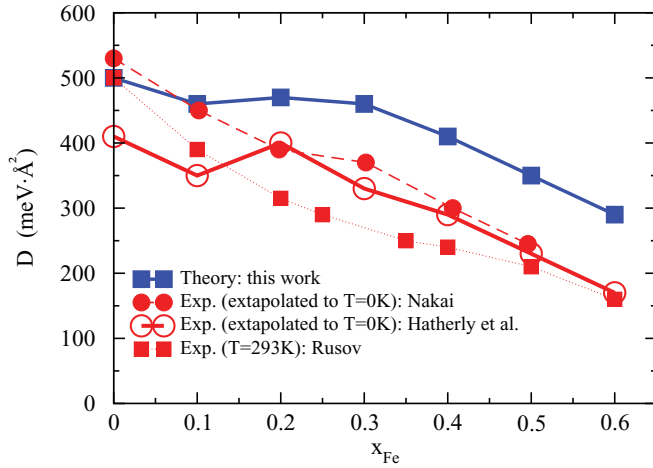


FIG. 3. (Color online) Spin stiffness constant of $\text{Fe}_x\text{Ni}_{1-x}$ alloys as a function of the concentration in comparison with experiment: Nakai²² (filled circles), Hatherly *et al.*²³ (open circles), and Rusov²⁴ (filled squares).

of the FM state. As can be seen from Fig. 4(b), around $\vec{q} = \vec{0}$ the individual Fe and Co moments are aligned parallel with respect to each other. However, after crossing $\vec{q}_c \approx \frac{\pi}{a}(0,0,0.7)$, the total magnetic moment jumps from $m = 1.46\mu_B$ to $m = 0.47\mu_B$ due to a change of the sign of the Co magnetic moment with respect to that of the dominating Fe moment. As Fig. 4(b) shows, the dispersion of the spin spiral energy for the antiparallel configuration gets very weak up to $\vec{q} \approx \frac{\pi}{a}(0,0,1)$. To estimate the energy of the spin spirals for the nonequilibrium configurations, i.e., antiparallel for $\vec{q}_c < \frac{\pi}{a}(0,0,0.7)$ and parallel for $\vec{q}_c > \frac{\pi}{a}(0,0,0.7)$, frozen potential calculations have been performed. The corresponding results are represented in Fig. 4(b) by dashed and dashed-dotted lines. Obviously, these results augment the two stable branches fairly well.

3. The disordered alloy $\text{Fe}_{0.5}\text{Mn}_{0.5}$

Figure 5 shows the results of spin spiral calculations for $\text{Fe}_{0.5}\text{Mn}_{0.5}$ having a noncollinear magnetic structure as a ground state.^{32–34} As is seen in the energy dispersion curve, Fig. 5(a), the system exhibits the behavior of a FM system

for wave vectors \vec{q} up to $\vec{q}_c \approx \frac{\pi}{a}(0,0,0.6)$. In this wave vector region the alloy has a small average magnetic moment formed by two antiparallel aligned magnetic moments of Fe and Mn occupying randomly the site [see Fig. 5(b)].

At $\vec{q}_c \approx \frac{\pi}{a}(0,0,0.6)$ the energy of a spin spiral reaches its maximum and the following increase of the wave vector is accompanied by a decrease in energy and an increase of the average magnetic moment. At $\vec{q} = (0,0,\frac{\pi}{a})$ the spin spiral magnetic structure reaches its energy minimum, which is about 50 meV lower than the energy of the FM state, with a parallel alignment of the magnetic moments of the alloy components.

Similar to $\text{Fe}_{0.5}\text{Co}_{0.5}$, these two minima of the energy—around $\vec{q} = \vec{0}$ and around $\vec{q} = (0,0,\frac{\pi}{a})$ —are formed by two crossing branches of the spin spiral dispersion relation: One corresponds to an antiparallel alignment of the Fe and Mn magnetic moments (around the $\vec{q} = \vec{0}$) and another to their parallel alignment [around $\vec{q} = (0,0,\frac{\pi}{a})$], which have a crossing point at $\vec{q} \approx \frac{\pi}{a}(0,0,0.6)$.

Thus, from the analysis of the energetics of the spin spiral structures in $\text{Fe}_{0.5}\text{Mn}_{0.5}$, one can conclude that the system has in its magnetic ground state an antiparallel alignment of the magnetic moments of first neighbors, no matter whether the neighboring atoms are Fe or Mn.

B. Spin susceptibility

In the present section we will discuss another application of the technique presented above. As was shown by Sandratskii and Kübler,¹¹ spin spiral calculations can also be used to determine the longitudinal magnetic susceptibility χ , both for magnetic and nonmagnetic systems, as a function of the wave vector \vec{q} . This approach allows us in particular to avoid the use of perturbation theory. Adding a Zeeman term to the Hamiltonian corresponding to a small external helical magnetic field allows us to obtain the magnetic susceptibility from the induced magnetic moments. For the present calculations a Zeeman splitting $B_0 = 1$ meV has been used.

The present work deals with nonmagnetic systems, which have either a paramagnetic (AgPt), a ferromagnetic (Ni), or an antiferromagnetic (Cr) ground state. Since we are dealing with magnetic systems in an imposed paramagnetic state, their magnetic susceptibility gives us information on an instability with respect to magnetic ordering.

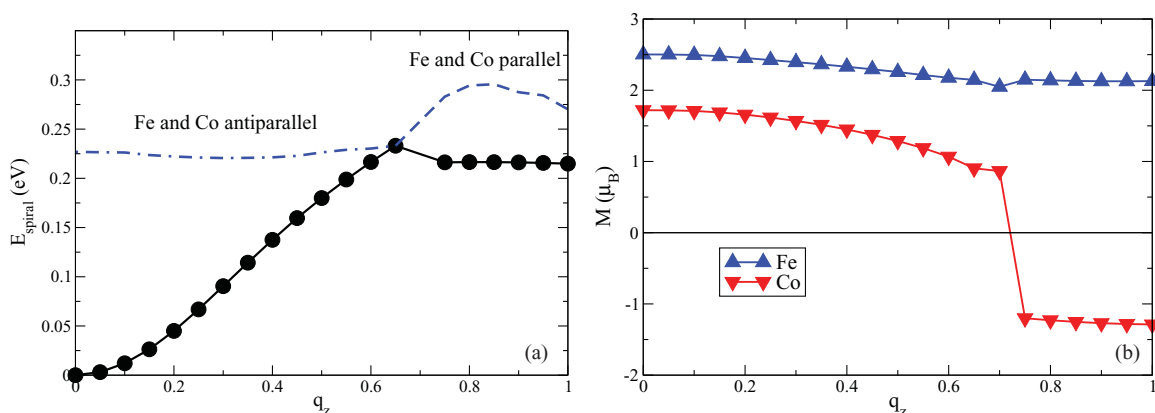


FIG. 4. (Color online) (a) The energy of spin spiral magnetic structure in $\text{Fe}_{0.5}\text{Co}_{0.5}$ calculated for the wave vector $\vec{q} = \frac{\pi}{a}(0,0,q_z)$ along the [001] direction. (b) Local magnetic moments on Fe and Co atoms separately, as a function of wave vector of spin spirals.

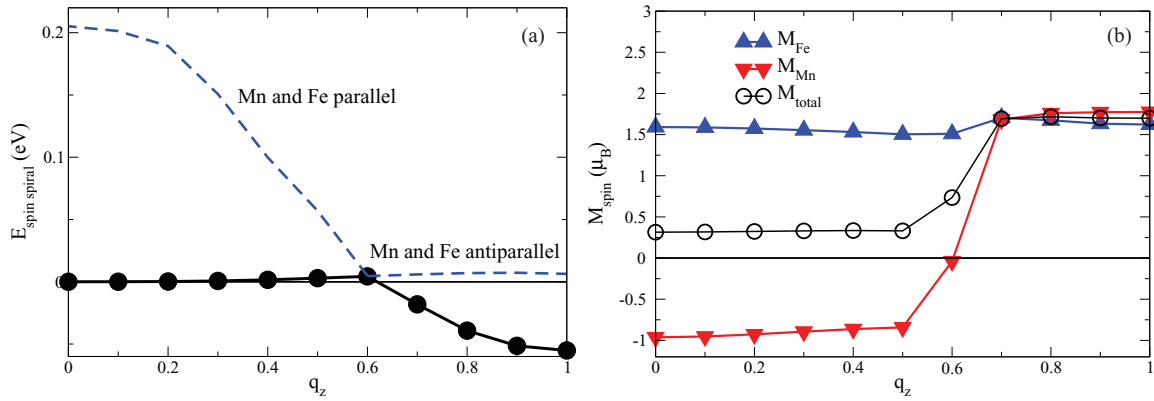


FIG. 5. (Color online) (a) The energy of spin spiral magnetic structure in $\text{Fe}_x\text{Mn}_{1-x}$ alloys calculated for the wave vector $\vec{q} = \frac{\pi}{a}(0,0,q_z)$ along the [001] direction. (b) Local magnetic moments on Fe and Mn atoms separately, as a function of wave vector of spin spirals.

1. The paramagnetic disordered alloy $\text{Ag}_x\text{Pt}_{1-x}$

Figure 6 shows the magnetic susceptibility of paramagnetic $\text{Ag}_x\text{Pt}_{1-x}$ alloys as a function of the wave vector \vec{q} for various concentrations. The spin susceptibility of the alloys presented in Fig. 6 is composed of contributions from both components according to $\chi(\vec{q}) = x\chi_{\text{Ag}}(\vec{q},x) + (1-x)\chi_{\text{Pt}}(\vec{q},x)$. For all concentrations, the increase of the wave vector for helical magnetic field is accompanied by a decrease of the response functions, as is usually found for paramagnetic systems. The main contribution to the spin susceptibility stems from the Pt atoms. As can be seen, increasing the Ag content leads to a decrease of the magnetic susceptibility for all values of wave vector.

The present results for $\vec{q} = \vec{0}$ are compared with the total magnetic susceptibility obtained via fully relativistic linear response calculations.²¹ As one can see, the agreement of results obtained by the two rather different theoretical approaches is rather good. One reason for the observed deviations is the use of a finite value for the external magnetic field in the present calculations giving the magnetic susceptibility from the induced magnetic moment within the self-consistent calculations. Another reason is the neglect

of spin-orbit coupling within the present calculations that usually reduces the spin susceptibility. Nevertheless, both approaches lead obviously to coherent results that are in rather satisfying agreement with experimental results³⁵ [filled squares in Fig. 6(b)]. Note however that experimental results represent the total magnetic susceptibility including also the orbital contribution.

2. Pure ferromagnetic fcc Ni

The calculations performed for ferromagnetic Ni in a paramagnetic state show a behavior for the magnetic susceptibility as a function of the wave vector that is rather different from that of systems with a paramagnetic ground state as for example $\text{Ag}_x\text{Pt}_{1-x}$ alloys (see Fig. 7). The paramagnetic state of Ni was simulated using the disordered local moment (DLM)³⁶ method assuming equal concentration for atoms with opposite orientation of their magnetic moments. The magnetically disordered state of Ni is characterized by a vanishing local magnetic moment and therefore the DLM method allows us to force the local magnetic moment to be zero. Figure 7(a) shows the results obtained for Ni with the experimental lattice parameter $a = 6.65$ a.u. At small values of the wave vector \vec{q}

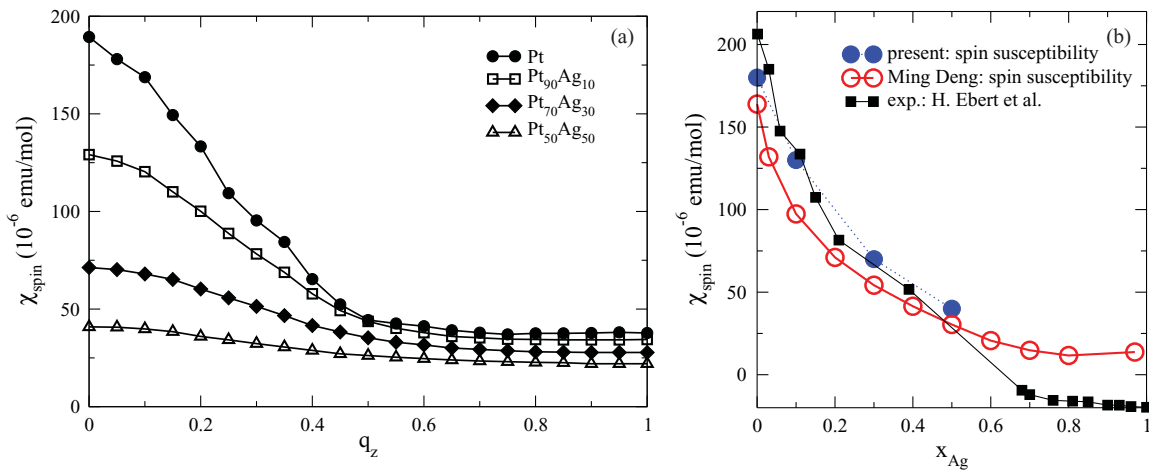


FIG. 6. (Color online) (a) Wave-vector $[\vec{q} = \frac{\pi}{a}(0,0,q_z)]$ dependent magnetic susceptibility of the paramagnetic disordered $\text{Ag}_x\text{Pt}_{1-x}$ for various concentrations. (b) Comparison of the present results for the susceptibility for $q = 0$ with the results of Deng et al.²¹ obtained via linear response theory.

the magnetic susceptibility is negative indicating an instability of the paramagnetic state. This is a result of the high density of states (DOS) of the 3d electrons leading to a large value of the unenhanced magnetic susceptibility χ^0 . Accordingly, for

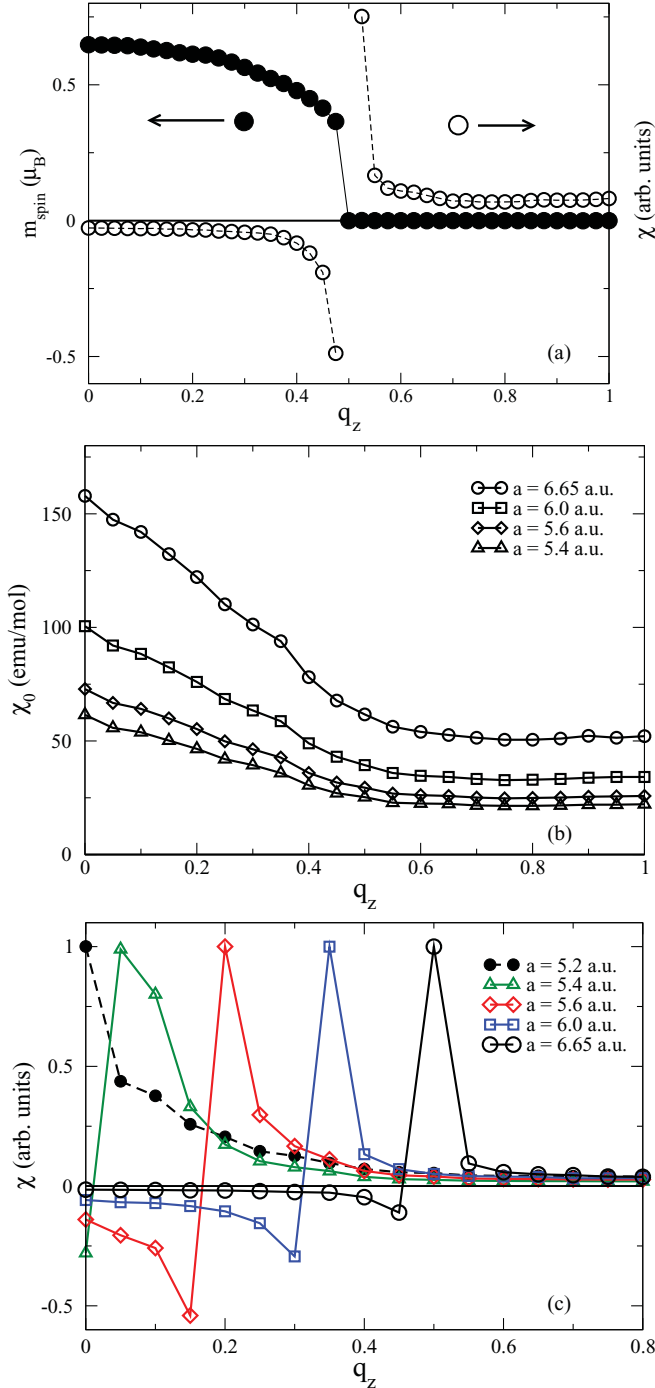


FIG. 7. (Color online) Wave-vector dependent [$\vec{q} = \frac{\pi}{a}(0,0,q_z)$] spin susceptibility of paramagnetic Ni having lattice parameter $a = 6.65$ a.u. together with local Ni magnetic moment as a function of wave-vector characterizing noncollinear spiral magnetic structure (a). The wave-vector dependent unenhanced (b) and enhanced (c) magnetic susceptibilities for paramagnetic Ni calculated for different lattice parameters.

small \vec{q} vectors the Stoner condition for a magnetic instability $I(\vec{q})\chi^0(\vec{q}) > 1$ [Eq. (17); see, e.g., Refs. 37 and 38] is fulfilled.

As one can see in Fig. 7, at the wave vector $\vec{q} \approx \frac{\pi}{a}(0,0,0.55)$ [for which the denominator in Eq. (17) comes to 0] the magnetic susceptibility becomes singular and the following increase of \vec{q} results in a change of sign for the susceptibility from negative to positive leading to the stability of the paramagnetic state.

Figure 7(a) shows also the Ni magnetic moment as a function of the wave vector \vec{q} of spin spiral. As one can see, the magnitude of the moment goes down upon increase of \vec{q} reaching $m = 0$ at the critical value of the wave vector \vec{q}_c .

As shown in Fig. 7(b), a decrease of the lattice parameter leads to a decrease of the unenhanced susceptibility $\chi(\vec{q})$ due to the broadening of the energy bands of the 3d states. This results in a decrease of the critical wave vectors \vec{q}_c until a lattice parameter is reached for which $\vec{q}_c = 0$. For smaller lattice parameters the ground state of Ni is the PM state.

3. Pure antiferromagnetic bcc Cr

Results for the nonmagnetic state of Cr having the AFM structure as a ground state are shown in Fig. 8. Note that

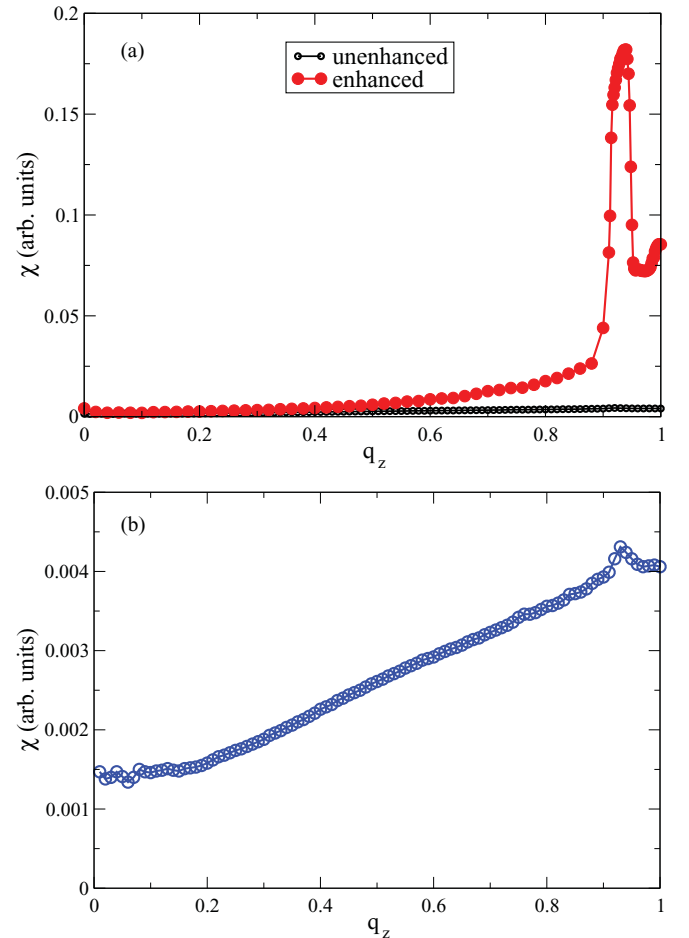


FIG. 8. (Color online) Wave-vector dependent [$\vec{q} = \frac{\pi}{a}(0,0,q_z)$] enhanced (a) and unenhanced (b) spin susceptibilities of paramagnetic Cr. For comparison, the unenhanced susceptibility is plotted also in panel (a).

the antiferromagnetic order of Cr on the one side is a result of the nearly half filling of the d band³⁷ (similar to Mn), which should result in a commensurate AFM structure. However, Cr exhibits also an instability with respect to an incommensurate spin-density wave (SDW) with the wave vector $\vec{q} \approx \frac{\pi}{a}(0,0,0.95)$, which is a result of the Fermi surface nesting. This leads to a singularity of the magnetic susceptibility at $\vec{q} \approx \frac{\pi}{a}(0,0,0.95)$ of paramagnetic Cr. This SDW instability in Cr and the corresponding behavior of the momentum dependent magnetic susceptibility was discussed in the literature by several authors.^{39–41}

Our present results demonstrate that the calculation of the momentum-resolved magnetic susceptibility properly reproduces its \vec{q} dependent features for Cr. The calculations have been performed for a lattice parameter $a = 5.4$ a.u. which is slightly smaller than the experimental one ($a \approx 5.44$ a.u.). At this lattice parameter the PM state was found to be more stable than the AFM state. This allows us to observe the behavior of $\chi(\vec{q})$ due to the Fermi surface nesting, avoiding the influence of other singularities connected to the instability around $\vec{q} = \pi/a(0,0,1)$ with respect to the AFM state.

Figure 8(b) shows a monotonous increase of the enhanced susceptibilities with increasing wave vector \vec{q} reaching its maximum at $\vec{q} \approx \pi/a(0,0,0.92)$. The enhanced susceptibility, also increasing with wave vector \vec{q} , has a drastic increase at $\vec{q} \approx \pi/a(0,0,0.92)$ due to the enhancement factor [Eq. (17)], which is associated with a singularity caused by the Fermi surface nesting mentioned above.

Here, we do not discuss the q dependence of the exchange integral $I(\vec{q})$ as this was done in detail by Sandratskii and

Kübler. Nevertheless, we would like to stress that this feature is taken into account within the self-consistent calculations for every wave vector. In fact this is essential for the analysis of the stability of the paramagnetic state.

IV. CONCLUSION

A theoretical approach for electronic structure calculations on systems with spiral magnetic structures within the KKR Green's function formalism has been presented. As has been demonstrated, by making use of symmetry, the scattering path operator can be obtained by solving the corresponding equation of motion in the reciprocal space. Compared to the case of collinear magnetic structure, the only structural Green's function to be used involves the wave vector of the spin spiral. As the KKR formalism combined with the CPA allows one to deal with chemically disordered materials, corresponding spin spiral investigations on various disordered alloys could be performed. In particular the energy of spin spirals and the behavior of the magnetic moments of the alloy components were analyzed. In addition it was shown that the approach presented can be efficiently used for the calculation of the momentum resolved longitudinal magnetic susceptibilities of pure materials as well as those of disordered alloys.

ACKNOWLEDGMENTS

This work was supported by the DFG within Project No. Eb 154/20, "Spin polarization in Heusler alloy based spintronics systems probed by SPINXPES."

-
- ¹L. M. Sandratskii, Phys. Status Solidi B **136**, 167 (1986).
²L. M. Sandratskii, J. Phys. Condens. Matter **3**, 8565 (1991).
³W. F. Brinkman and R. J. Elliot, Proc. R. Soc. London A **294**, 343 (1966).
⁴W. F. Brinkman and R. J. Elliot, J. Appl. Phys. **37**, 1457 (1966).
⁵C. Herring, in *Magnetism*, edited by G. Rado and H. Suhl (Academic Press, New York, 2000), Vol. IV, p. 191.
⁶L. M. Sandratskii, Adv. Phys. **47**, 91 (1998).
⁷O. N. Mryasov, A. I. Liechtenstein, L. M. Sandratskii, and V. A. Gubanov, J. Phys. Condens. Matter **3**, 7683 (1991).
⁸S. V. Halilov, H. Eschrig, A. Y. Perlov, and P. M. Oppeneer, Phys. Rev. B **58**, 293 (1998).
⁹N. M. Rosengaard and B. Johansson, Phys. Rev. B **55**, 14975 (1997).
¹⁰J. Kübler, *Theory of Itinerant Electron Magnetism* (Oxford University Press, Oxford, 2000), p. 460.
¹¹L. M. Sandratskii and J. Kübler, J. Phys. Condens. Matter **4**, 6927 (1992).
¹²J. B. Staunton, J. Poulter, B. Ginatempo, E. Bruno, and D. D. Johnson, Phys. Rev. B **62**, 1075 (2000).
¹³T. Jarlborg, Solid State Commun. **57**, 683 (1986).
¹⁴P. Strange and B. L. Gyorffy, J. Phys. F **16**, 2139 (1986).
¹⁵M. Uhl, L. M. Sandratskii, and J. Kübler, Phys. Rev. B **50**, 291 (1994).
¹⁶H. Ebert, in *Electronic Structure and Physical Properties of Solids*, Vol. 535 of Lecture Notes in Physics, edited by H. Dreyssé (Springer, Berlin, 2000), p. 191.
¹⁷M. Matsumoto, J. B. Staunton, and P. Strange, J. Phys. Condens. Matter **2**, 8365 (1990).
¹⁸W. H. Butler, Phys. Rev. B **31**, 3260 (1985).
¹⁹D. Ködderitzsch, H. Ebert, D. A. Rowlands, and A. Ernst, New J. Phys. **9**, 81 (2007).
²⁰A. Zunger, S.-H. Wei, L. G. Ferreira, and J. E. Bernard, Phys. Rev. Lett. **65**, 353 (1990).
²¹M. Deng, Ph.D. thesis, University of Munich, 2001.
²²I. Nakai, J. Phys. Soc. Jpn. **52**, 1781 (1983).
²³M. Hatherly, K. Hirakawa, R. D. Lowde, J. F. Mallett, M. W. Stringfellow, and B. H. Torrie, Proc. Phys. Soc. London **84**, 55 (1964).
²⁴G. I. Rusov, Sov. Phys. Solid State **9**, 146 (1967).
²⁵K. Terakura, N. Hamada, T. Oguchi, and T. Asada, J. Phys. F **12**, 1661 (1982).
²⁶H. Hasegawa, J. Phys. F **14**, 1235 (1984).
²⁷A. V. Ruban, S. Khmelevskyi, P. Mohn, and B. Johansson, Phys. Rev. B **75**, 054402 (2007).
²⁸A. I. Liechtenstein, M. I. Katsnelson, and V. A. Gubanov, J. Phys. F **14**, L125 (1984).
²⁹M. Pajda, J. Kudrnovský, I. Turek, V. Drchal, and P. Bruno, Phys. Rev. B **64**, 174402 (2001).
³⁰M. van Schilfgaarde and V. P. Antropov, J. Appl. Phys. **85**, 4827 (1999).
³¹O. N. Mryasov, A. J. Freeman, and A. I. Liechtenstein, J. Appl. Phys. **79**, 4805 (1996).

- ³²T. C. Schulthess, W. H. Butler, G. M. Stocks, S. Maat, and G. J. Mankey, *J. Appl. Phys.* **85**, 4842 (1999).
- ³³D. D. Johnson, F. J. Pinski, and G. M. Stocks, *J. Appl. Phys.* **63**, 3490 (1988).
- ³⁴Y. Endoh and Y. Ishikawa, *J. Phys. Soc. Jpn.* **30**, 1614 (1971).
- ³⁵H. Ebert, J. Abart, and J. Voithländer, *J. Phys. F* **14**, 749 (1984).
- ³⁶B. L. Gyorffy, A. J. Pindor, J. Staunton, G. M. Stocks, and H. Winter, *J. Phys. F* **15**, 1337 (1985).
- ³⁷T. Moriya, *Spin Fluctuations in Itinerant Electron Magnetism* (Springer, Berlin, 1985).
- ³⁸P. Mohn, *Magnetism in the Solid State* (Springer, Berlin, 2003), p. 215.
- ³⁹J. B. Staunton, J. Poulter, B. Ginatempo, E. Bruno, and D. D. Johnson, *Phys. Rev. Lett.* **82**, 3340 (1999).
- ⁴⁰D. J. Crockford and W. Yeung, *Comput. Phys. Commun.* **75**, 55 (1993).
- ⁴¹E. Fawcett, *Rev. Mod. Phys.* **60**, 209 (1988).